Mechatronics 22 (2012) 1177–1186

Contents lists available at SciVerse ScienceDirect

Mechatronics

journal homepage: www.elsevier.com/locate/mechatronics

Direct design of a velocity controller and load disturbance estimation for a self-balancing industrial manual manipulator

Fabio Previdi [a,*], Federico Fico [a], Sergio M. Savaresi [b], Damiano Belloli [a,b], Ivan Pesenti [c]

[a] Dipartimento di Ingegneria dell'Informazione e Metodi Matematici, Università degli Studi di Bergamo, Via. Marconi 5, 24044 Dalmine, BG, Italy
[b] Dipartimento di Elettronica e Informazione, Politecnico di Milano, p.zza Leonardo da Vinci 32, 20133 Milano, MI, Italy
[c] Scaglia Indeva spa, via Marconi 42, 24012 Brembilla, BG, Italy

ARTICLE INFO

Article history:
Received 11 October 2011
Accepted 13 October 2012
Available online 10 November 2012

Keywords:
Velocity control
Direct controller design
Load estimation

ABSTRACT

Self-balancing manual manipulators are devices that countervail the weight of a load that must be manually handled and moved by a human operator. Standard manipulators are made of a framework with an electric motor on the top and a spool connected to the motor shaft through a transmission gear. The load is hung by a handling device connected to a metallic rope wound on the spool. The device considered in this paper, in its current layout, is endowed with a load cell that measures the load weight and is controlled in an open loop. A new layout has been designed, which is not including the weighting load cell and is feedback controlled. The load's counterbalance and movement are obtained by a velocity closed loop control algorithm designed using a direct design method, the Virtual Reference Feedback Tuning (VRFT). VRFT provides controller parameters tuning in a completely automatic way based on a single I/O batch measurement on the plant. Moreover, the elimination of the load weight transducer causes issues to some handling devices that need weight measurements to attach and detach the load. So, a load mass observer has been designed using a gravitational torque estimator, which is an enhanced version of standard disturbance torque observer for electric motors.

1. Introduction and problem statement

Self-balancing manual manipulators are devices devoted to help human operators in manually handling heavy loads. Such systems are composed by a mechanical structure, that can be different depending on the application, and a controlled DC electric motor attached to it. The motor shaft is connected to a spool by means of a transmission gear. The load is hooked to a handling device positioned at the end of a metallic rope wound on the spool. The electric motor produces the torque necessary to balance the weight of a load, so that a human operator can manually handle and move it as if it were virtually weightless. These devices have both the flexibility of a human operator and the power of a machine and are used in many different industrial sectors, where the complexity of the positioning, the difficulty of movements in a work area or the peculiarity of the load to be moved need human direct operations.

Before this research project, the functioning of the manipulator considered in this work was based on a very simple principle. The device used to be endowed with two load cells: the first one measuring the load weight, so that the motor, based on such information, could generate the mechanical torque needed to balance the weight; the second, positioned on the handle grasped by the operator, measuring the force impressed to the system, so that the motor could generate an additional torque to make the load movement easier. This operation scheme has been chosen in the past since the load weight could strongly vary during normal operations; but it presents various drawbacks, the main of which is low robustness to the load weight cell measurement errors which occasionally result in spontaneous undesired drift motion of the load.

In this paper we present the development of a new prototype device without the balancing load cell and provided with a closed-loop velocity controller for the electric motor. The idea is to generate a velocity reference signal using the handle load cell and to feed it into the closed loop system, which will certainly present robustness to load weight variations. The elimination of one load cell has a non-negligible effect on the device cost and eliminate some undesired behaviors of the manipulator, reducing the maintenance needs. Moreover, it offers the chance of a software personalization of the operator feelings during the load movements, with a strong impact also on the safety of the worker.

The design of the new control system presents two main issues:

(1) On the first hand, each manipulator controller is normally fine-tuned at the end of the production line for best performance. So, a completely automatic auto-tuning procedure for the velocity control loop is strongly advisable.

* Corresponding author. Tel.: +39 0352052357; fax: +39 0352052300.
E-mail addresses: previdi@unibg.it (F. Previdi), savaresi@elet.polimi.it (S.M. Savaresi), ivan.pesenti@it.indevagroup.com (I. Pesenti).

0957-4158/$ - see front matter © 2012 Elsevier Ltd. All rights reserved.
http://dx.doi.org/10.1016/j.mechatronics.2012.10.003

(2) Secondly, some handling devices need the load weight measure to be correctly operated. Since the new manipulator layout no longer has a physical transducer for load weight measurement, a load weight observer has to be designed, in order to obtain mass estimates instead of weight measures.

The first problem has been solved resorting to a direct control design approach: the *Virtual Reference Feedback Tuning* (VRFT) strategy, which allows the tuning of a feedback controller without having a model of the plant [1,2]. The VRFT method gives a solution to the problem of designing a controller for a system on the basis of a single set of I/O data. So, this algorithm is strongly appealing in view of the design of an end-of-line auto-tuning procedure of the self-balancing control algorithms and, in general, in any industrial application. The idea on which VRFT is based was originally proposed in [1–3] and developed in [4–7]. Then, it has been realized in its final form, used in this paper in [6,7], as a complete and ready to use method for data-driven control design in a noisy environment. Also, VRFT has successfully found a number of applications, from automotive [8] to biomedical [9,10] and electro-hydraulic actuators control problems [11]. Also Iterative Feedback Tuning (IFT) could be a promising data-driven model-free control technique for this application. The control design is based on the minimization of a control criterion with respect to the controller parameters using an iterative gradient technique. In [12] an interesting solution for nonlinear system is proposed. In [13] a similar method is applied to robotic manipulators and in [14] a solution is presented for a case study very similar to the one tackled in the present paper. What we experienced in practice is a critical dependence on the reference signal features and a computational load problem, but the use of IFT techniques will certainly be the object of further studies.

The second issue has been tackled starting from standard disturbance torque observer algorithms for electric motors [15–18] or robotic applications [19,20]. Usually, the torque disturbance is estimated in view of its compensation, or the reaction torque is computed to perform sensorless force control. In this work, an algorithm to estimate the varying gravitational disturbance torque has been developed and implemented on the new manipulator.

The paper is organized as follows: in Section 2 the experimental set up is outlined and the architecture of the new control system is described and compared with the old one. Section 3 is devoted to a short description of the VRFT approach, and the experimental results, showing the closed loop control system performance, are presented in Section 4. Similarly, Section 5 presents the design and

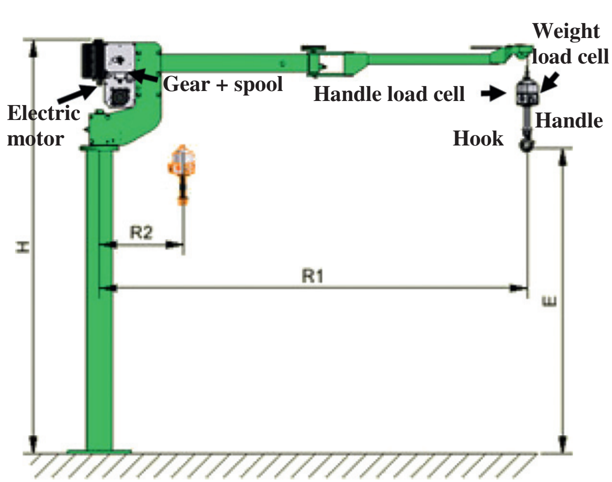

Fig. 1. Schematic representation of the device used in this work.

Fig. 2. Example of operating condition of the device in food industry. Notice that the manipulator in this picture is equipped with a suction-pad: vacuum is done inside the pad by a pneumatic compressor, the load is attached to the handling device and can be moved.

tuning of the load weight observer, and Section 6 shows the estimator performance in comparison with load cell measurements.

2. Experimental setup

A schematic representation of the device considered in this paper is shown in Fig. 1 (a picture is shown in Fig. 2). The manipulator is made by five main parts:

(1) A *mechanical structure*, specifically designed for the operating needs of the end user. In the present paper, we performed experiments on a free-standing column with a folding arm (other different supports are available such as ceiling support, overhead rails or jibs). The fully extended arm is 2 m long and the column height is 2.43 m.

(2) A *DC brushed electric motor* (about 500 W power), placed at the top of the column; the motor is endowed only with an embedded closed loop current controller.

(3) A *two-stage motion transmission system* composed by a gear wheel and a belt drive, with overall transmission ratio $n = 20$. Rotation speed is measured by an encoder positioned on the first spool rotation shaft. Motion is transmitted from the motor shaft to a steel rope wound on a spool.

(4) A *steel rope* wound on the spool and supporting the handling device. The rope will be supposed perfectly inextensible.

(5) A *handle* holding the load positioned at the end of the rope. The handle is a complex mechanical device endowed with two load cells, which measure, respectively, the forces delivered by a human operator and the load weight. The elimination of the weighting load cell is one of the goals of the present paper. The handle can be equipped with many different handling tools. In this work, the experiments about velocity control design have been performed using a hook with total weight (handle + hook) of about 7 kg. The mass estimator has been also tested in more critical conditions using a pneumatic handling system of about 20 kg weight. The manipulator considered in this paper is designed to lift a maximum load of 80 kg.

The development of all the algorithms described in the following sections has been done by means of a rapid prototyping system by National Instruments, including the software development tool Labview and two hardware devices: the CompactDAQ system and the Compact Real I/O system for real-time implementation of the control and estimation algorithms. Final implementation has been done on the device control board based on Freescale Motorola 56F8300. All the signals used in this paper have been sampled at 200 Hz.

Before the development of the research project described in this paper, the electric motor was driven in an *open loop* (see Fig. 3). The total current I_{tot} driving the motor was the sum of two contributions:

(1) The first one, namely I_l, set proportional (through a design coefficient C_l) to the load measurement was actually a *balancing current*: its effect was a torque, produced by the motor, which balanced the load, whose effect on the motor shaft was a disturbance torque T_l.
(2) The second one, namely I_h, set proportional (through a design coefficient C_h) to the handle load cell measurement, produced the additional torque needed to move the load. So, the operator applied force on the handle, which was measured by the handle load cell and transformed into torque at the motor shaft.

As evident from Fig. 3, the control architecture was a standard open loop compensation of a measurable load. Using this control scheme we experienced low robustness to the load cell measurement errors. This drawback was only partially compensated by the large static friction of the motor–gear–spool system and occasionally some device presented spontaneous undesired drift motion.

So, a new *closed loop* control system has been designed according to the scheme of Fig. 4. The load disturbance compensation is provided by a closed-loop velocity 1-DOF controller, based on the rotation speed measurement v provided by the electric motor encoder. This control architecture is intrinsically more robust to any external disturbance, and in particular to load disturbances, without any need of measuring it: in fact, the weight load cell can be eliminated. The reference signal v_{ref} of the velocity control loop is generated by a suitable filtering of the handle load cell measurement. The tuning of the velocity controller has been done resorting to the VRFT approach, which is a completely automatic tuning procedure based on a single batch I/O measurement performed on the plant (see Sections 3 and 4). This way, the controller tuning can be done at the end of the production line quickly and without human direct intervention. It is worth noting that the VRFT tuning can also be applied to maintenance during the manipulator life-time, if some significant modification of its dynamical behavior occurs (for instance, dynamic friction reduction, changes in the motor efficiency, etc.).

In some applications (mainly those involving pneumatic handling devices), the value of the load weight must be known. Since in the new version of the device the weight load cell has been eliminated, a "software load sensor" has been developed, i.e. an algorithm which estimates the load weight value using the available measurements: current and velocity (see Sections 5 and 6).

3. Velocity control loop: Virtual Reference Feedback Tuning (VRFT)

The VRFT strategy [7] approximately solves a model-reference problem in a discrete time. The control specifications are assigned via a reference model, which describes the desired behavior of the closed-loop system. The reference model is given in terms of a transfer function $M(q)$, being q^{-1} the unit delay operator. This model is used to define, in a simple and effective way, the basic characteristics of the closed-loop control system, such as its settling time and the allowed overshoot. Typically, a first or second order model allows a complete specification of the closed loop performances [8–11].

The VRFT approach allows a "one-shot" tuning of a linear controller, i.e. the controller parameters are directly derived from a single batch of data without any specific action by the designer. This feature is very useful in the present application. In fact, using the VRFT algorithm, the end-of-line tuning of the controller can be performed in a very short time with great benefits for productivity.

In the VRFT approach the following closed-loop system is considered:

$$y(t) = P(q)u(t) \tag{1.1}$$

$$u(t) = C(q;\theta)(r(t) - y(t)) \tag{1.2}$$

The plant is described by its (unknown) transfer function $P(q)$, and $C(q;\,\theta)$ is the transfer function of a one-degree-of-freedom controller belonging to a given family of linear transfer function controllers $\{C(q;\theta)\}_{\theta\in\mathbb{R}^n}$ parameterized by the n-dimensional real vector θ. The signals $u(t)$ and $y(t)$ are respectively the input (the control action) and the output of the considered plant (assumed to be scalar). The signal $r(t)$ is the reference signal of the control loop. The closed loop system dynamic is characterized by the transfer function from $r(t)$ to $y(t)$:

$$y(t) = \frac{P(q)C(q;\theta)}{1 + P(q)C(q;\theta)}r(t) \tag{2}$$

Let us assume that a set of I/O data $\{u(t), y(t)\}_{t=1,\dots,N}$ has been collected during an experiment on the plant and that a reference model $M(q)$ has been chosen on the basis of the desired closed-loop behavior. If the plant model $P(q)$ were known, the controller $C(q;\,\theta)$ could be designed, i.e. a value for the parameter θ could be estimated, by solving the following model reference problem:

$$\hat{\theta} = \arg\min_{\theta} J_{MR}(\theta) \tag{3.a}$$

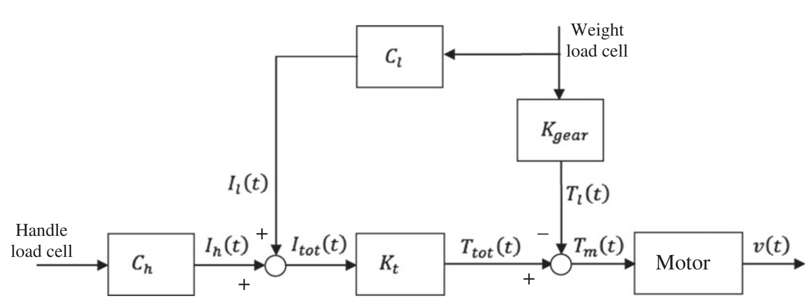

Fig. 3. Representation of the "old" open-loop control architecture. The parameter K_t represents the torque constant of the motor; the parameter K_{gear} is the transformation coefficient of the load cell measured force into the torque at the motor shaft. The block "Motor" represents the mechanical part of the electric motor.

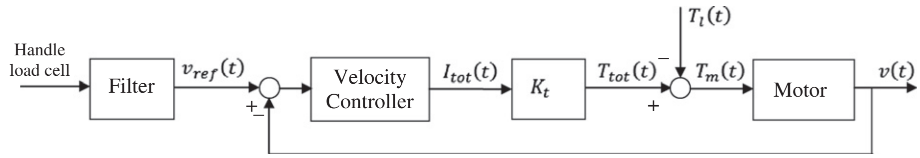

Fig. 4. Representation of the "new" closed-loop control architecture. Notice that the weight load cell disappeared.

where

$$J_{MR}(\theta) = \left\| \frac{P(z)C(z;\theta)}{1+P(z)C(z;\theta)} - M(z) \right\|_2^2 \tag{3.b}$$

By means of VRFT, it is possible to approximately solve this problem without knowledge of the plant transfer function. The idea is to transform the Model Reference (MR) problem into a Virtual Reference (VR) one, which can be proven to be approximately equivalent to the first one under mild conditions.

To this aim, given the measured $y(t)$ (i.e. the actual signal measured at the output of the plant), consider a *virtual reference* $r_v(t)$ such that $M(q)r_v(t) = y(t)$; $r_v(t)$ is called *virtual* because it does not exist in reality (it is not used in the generation of $y(t)$). In this framework, $y(t)$ is the desired output of the closed-loop system when the reference signal is $r_v(t)$ and the corresponding *virtual tracking error* is $e_v(t) = r_v(t) - y(t)$. In fact, even though the plant transfer function $P(q)$ is not known, when the plant is fed by $u(t)$ (the actually measured input), it generates $y(t)$ (the corresponding measured output). Therefore, a good controller must generate $u(t)$ when fed by $e_v(t)$ as an effect of the application of the *virtual reference* $r_v(t)$. The idea is to search for such a controller.

Since both signals $u(t)$ and $e_v(t)$ are known, this task reduces to the "*identification problem*" of describing the dynamical relationship between $e_v(t)$ and $u(t)$ by using the family of linear models $\{C(q;\theta)\}_{\theta\in\mathbb{R}^n}$, i.e. estimating

$$\hat{\theta} = \arg\min_{\theta} J(\theta) \tag{4.a}$$

by minimizing the following cost function

$$J(\theta) = \frac{1}{N}\sum_{t=1}^{N}(u(t) - C(q;\theta)e_v(t))^2 \tag{4.b}$$

Obviously, the minimization of the cost function (4) is not equivalent to the minimization of the original MR cost function (3). However, it is proven in [7] that a filter $L(z)$ can be designed so that the MR criterion (3) can be matched through the criterion (4) applied to filtered version of $u(t)$ and $e_v(t)$ (specifically, the minimum arguments of both criteria can be made as close as possible – even identical – in ideal conditions).

In the following, the algorithm implementing the above idea is briefly outlined. In the algorithm, the identification of the controller is addressed by applying the classical least-squares identification criterion [21–23].

Given the reference model $M(q)$, the family of controllers $\{C(q;\theta)\}_{\theta\in\mathbb{R}^n}$ and the set of data $\{u(t), y(t)\}_{t=1,\ldots,N}$ apply the following procedure:

1. Calculate:
   – a virtual reference $r_v(t)$ such that

     $y(t) = M(q)r_v(t)$, and

   – the corresponding virtual tracking error

     $e_v(t) = r_v(t) - y(t)$

2. Filter the signals $e_v(t)$ and $u(t)$ with a suitable filter $L(q)$, obtaining:

$$e_L(t) = L(q)e_v \tag{5.a}$$
$$u_L(t) = L(q)u(t) \tag{5.b}$$

3. Estimate the controller parameter vector

$$\hat{\theta} = \arg\min_{\theta} J_{VR}(\theta) \tag{6.a}$$

where

$$J_{VR}(\theta) = \frac{1}{N}\sum_{t=1}^{N}(u_L(t) - C(q;\theta)e_L(t))^2 \tag{6.b}$$

Notice that Eq. (6.b) is quadratic in the parameter vector θ and all the computations are directly performed on the measurement data, assumed that the filter $L(q)$ is given. The optimal filter (see [6]) to be used in the design is

$$L(z) = \frac{M(z)(1-M(z))}{U(z)} \tag{7}$$

where $U(z)$ is a model of the input signal such that $u(t) = U(q)\nu(t)$ where $\nu(t)$ is a white noise with unit variance, so that the power density spectrum of the input can be modeled as $\varphi_u(\omega) = |U(e^{j\omega})|^2$. The model used in this case is an AR(16). The system order has been estimated using MDL criterion [23].

Specifically, in this work, we consider the class of PI controllers, which are known to be effective in velocity control of DC electric motors [24]. The PI controller transfer function (in continuous time) depends only on two parameters

$$R(s) = K_i\frac{1+sT_i}{s} \tag{8.a}$$

where $K_i = \frac{K_p}{T_i}$, being K_p the proportional gain and T_i the integral time constant. The transfer function (8.a), opportunely discretized by backward integration, ends in a discrete time controller again depending on two parameters that must be tuned

$$\overline{R}(z) = \overline{K}_i\frac{1-\overline{T}_i z^{-1}}{1-z^{-1}} \tag{8.b}$$

Notice that, as already evidenced, since the controller is linear in the parameters $\theta = [\theta_1 \quad \theta_2] = [\overline{K}_i \quad \overline{K}_i\overline{T}_i]$, the performance index $J_{VR}(\theta)$ is quadratic in the parameters and an estimate $\hat{\theta}$ can be easily found.

4. Velocity control loop: experimental results

In this section, experimental results about the velocity control loop performances are presented. Specifically, in order to apply the VRFT algorithm, the first step is the design of an open loop experiment for the acquisition of the I/O data set. Experiments have been performed using a load weight of 47 kg, a medium weight with respect to the operating range of the manipulator (maximum load about 80 kg). The test input current is a band limited white noise sequence with frequency limit at 5 Hz. The mean value of the current has been set to 5.8 A, which is the value needed to balance the load. The experiment duration is 30 s. The output velocity is the vertical load speed computed using the measured spool rotation speed. The measured signals have been sampled with sampling frequency $f_s = 200$ Hz (see Fig. 5).

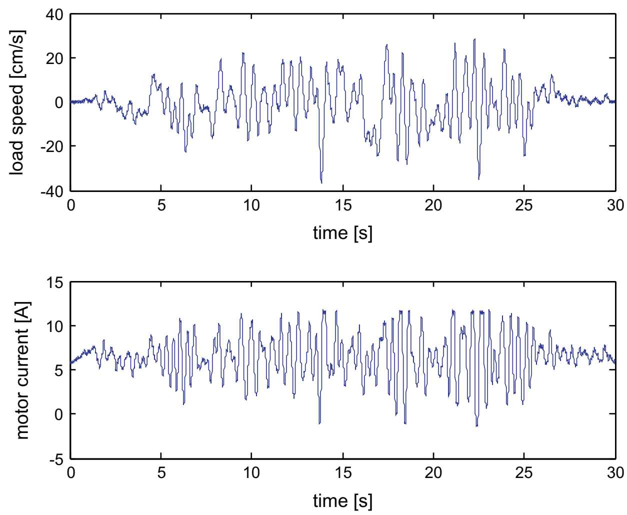

Fig. 5. I/O data set used for controller tuning.

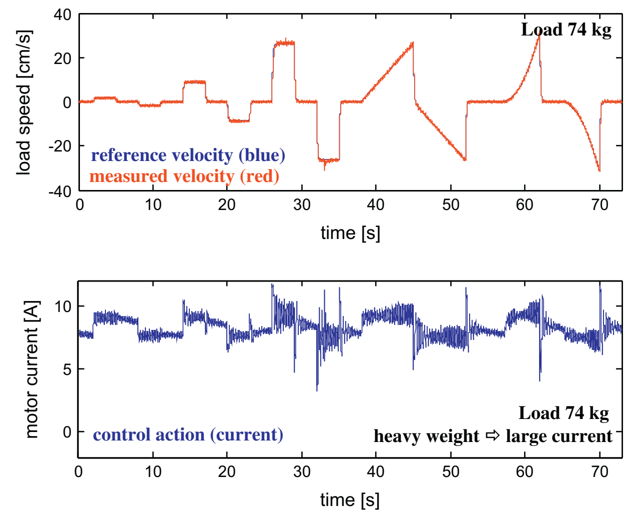

Fig. 7. Tracking experiment with heavy weight (notice the current mean value close to 8–10 A).

The reference model used to compute the virtual reference and to design the filter $L(z)$ is

$$M(z) = 0.556\frac{1+z^{-1}}{1+0.111z^{-1}}$$

This transfer function has been obtained by discretization of a first-order continuous time model with a unitary gain and a pole in ω = 500 rad/s. This is a quite fast model reference, in particular with respect to the sampling frequency, and the discrete time model has a pole in the left half plane. However, this is not significantly affecting the performance of the controller obtained (see Figs. 6 and 7), but for quite large control action values to counteract the poorly damped load oscillating disturbance. The minimization of the virtual reference cost function ends in the following parameter values (see Eq. (8.b)): $\overline{T}_i = 0.92$.

To evaluate the control performances, the tuned controller has been validated through two different experiments.

In the *first experiment*, a velocity reference signal has been computer-generated with the aim of rigorous testing the tracking ability of the control system. This experiment has been performed in two different conditions: with a light weight (7 kg, see Fig. 6) and a heavy weight (74 kg, Fig. 7). Remember that the controller has been designed with a medium weight (47 kg).

The reference signal is chosen as follows (see Figs. 6 and 7):

- square waves of different amplitude;
- ramp signals, both with positive and negative slope;
- parabolic signals, both with positive and negative concavity.

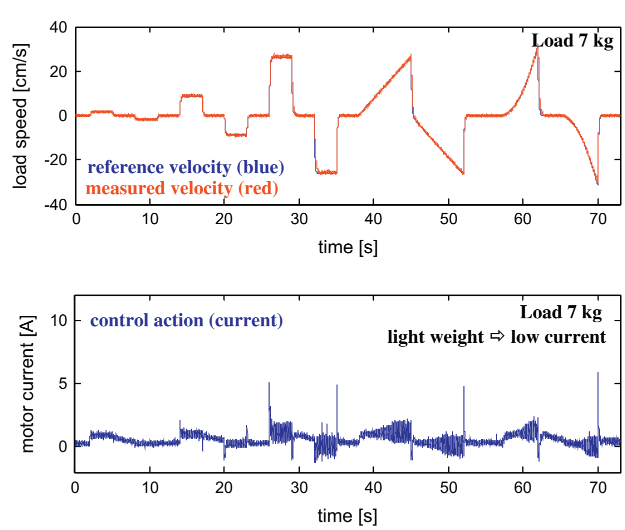

Fig. 6. Tracking experiment with a light weight (notice the current mean value in the range 0–1 A).

Both Figs. 6 and 7 present in the upper part the reference velocity and the measured velocity; in the lower part the electric motor current (control action). These experiments show that the controller, designed at a medium weight value, is able to provide very good tracking performances in the full operating range of the manipulator (0–80 kg). It is worth pointing out that the chosen reference signal severely tests the machine, with acceleration requests close to the motor power limit. As a result, during the movement, the mass is subject to poorly damped large oscillations, in particular in the case of large mass values, causing large variations in the torque load disturbance signal (see Fig. 4). The controller is fast enough to compensate for such oscillations, at the price of using oscillating large control action values, as expected.

The use of a slower controller, achievable by defining a slower model reference, has been also considered. However, it did not obtain the approval of the operators devoted to the test of the device. In fact, with a slower controller, the operators experienced a bad "feeling" in using the manipulator: they feel that the load was not following quickly enough their commands.

An example of the *second experiment* is shown in Fig. 8. In this case, a human operator is manually driving the manipulator in normal operating conditions with a heavy weight (74 kg). Specifically, referring to Fig. 8:

- in the upper figure, the handle load cell measurement is shown: this is a measure of the force impressed by the operator on the handle, i.e. the desired motion direction and acceleration.
- the velocity reference signal (blue[1] line – middle figure), which is carefully tracked by the control system (red line – middle figure), is generated by suitably filtering the handle force measure
- the bottom figure shows the current supplied to the electric motor.

[1] For interpretation of color in Figs. 8, 11, 13, and 14, the reader is referred to the web version of this article.

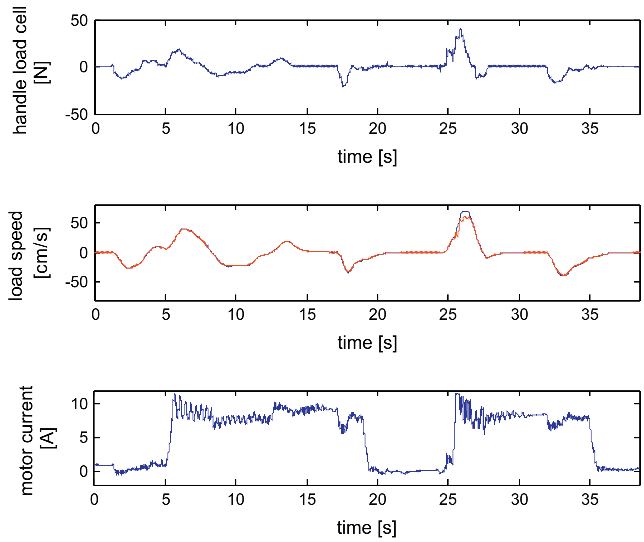

Fig. 8. Tracking experiment in normal operating conditions; the manipulator is driven by a human operator with a 74 kg load.

Notice that, after about 25 s, the tracking is not perfect, since the motor power limit is reached, which is evident from the saturation of the current signal. This kind of test has been performed by many different operators, and all of them report great satisfaction about the manipulator handling.

Finally, it is worth making some remarks about the use of the VRFT algorithm in this specific application:

(1) The VRFT tuning procedure is robust in the use of different instances of the I/O data (but using the same reference model and load weight): basically, it provides the same parameter tuning (within about 2% about the mean values).
(2) Obviously, the application of the algorithm with different load values provides different values of the controller parameters. For instance, if a heavy weight is used to collect the I/O data for the VRFT, the tracking performance will be slightly lower than at a light weight, because the controller gain will be larger than needed. Similarly, if a light weight is used for tuning, the control system will be slower because of a smaller controller gain.
(3) The controller characteristics, in terms of closed loop response, can be easily driven by a wise choice of the model reference system and can be changed according to any designer specification.

5. Load weight estimator: design and tuning

As pointed out in Section 1, the new self-balancing manipulator endowed with the velocity control loop no longer needs the load weight measurement to perform movement control. However, the manipulator can be equipped with different handling tools, some of which need the weight load information to be operated. So, a load mass observer has been developed to estimate the load weight $\widehat{M}$ based on the other available measures, i.e. the current I and the motor speed velocity ω.

The mass can be calculated by estimating the gravitational component of the disturbance torque acting on the DC motor. Disturbance torque estimation is a well known issue in literature (see [15–20] as examples). Two main issues are usually considered: the estimation of the total disturbance torque for its compensation (see [15–18] as examples) and the estimation of the reaction torque for sensorless control (see [19,20] as examples). In the first case it is not necessary to distinguish the various contributions to the disturbance torque. In the second case, it is necessary to distinguish between the reaction torque by gravity and friction, which are usually jointly estimated offline, since they are constant in most applications. On the contrary, in this application, the gravity torque must be estimated separately, and it can be highly variable, since the load weight can vary during normal operations.

Specifically, the system can be modeled as follows:

$$J\dot{\omega}(t) = T(t) - T_v(t) - T_c - T_g(t) \tag{9}$$

On the left hand side of Eq. (9), J is the total inertia moment. On the right hand side, $T(t) = K_t I(t)$ is the DC motor torque, being K_t the motor torque constant; $T_v(t) = D\omega(t)$ is the viscous friction torque; T_c is the Coulomb friction torque, and the last term $T_g(t)$ is the gravitational torque that we want to compute. Notice that there is no reaction torque in this application.

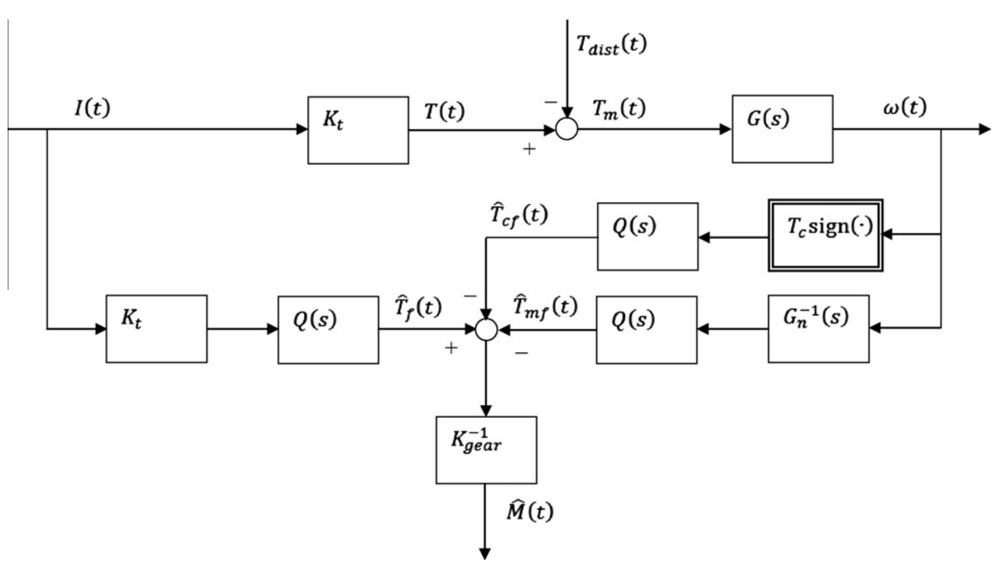

Fig. 9. General scheme of the load mass observer.

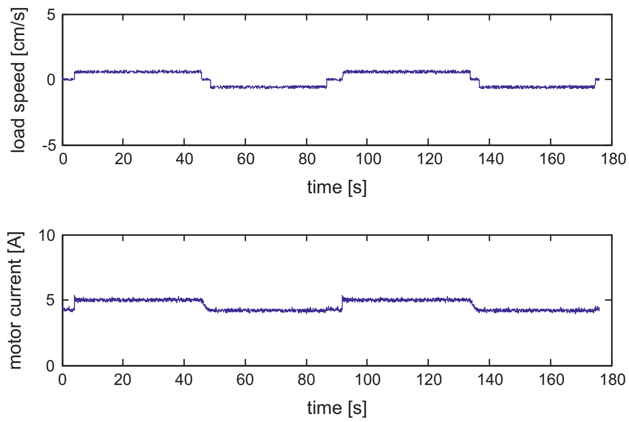

Fig. 10. Example of one of the experiments (39 kg load) used to estimate Coulomb friction effects.

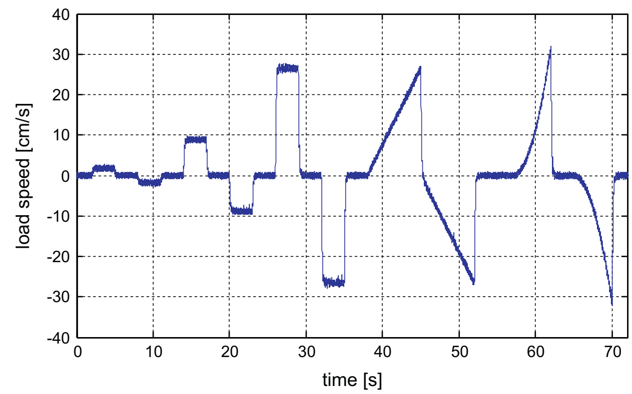

Fig. 12. Velocity reference signal used for observer performance evaluation.

Table 1
Estimated Coulomb friction torque at different load values.

Load weight (kg)	T_C (N m)
14	0.0807
39	0.1189
74	0.1982

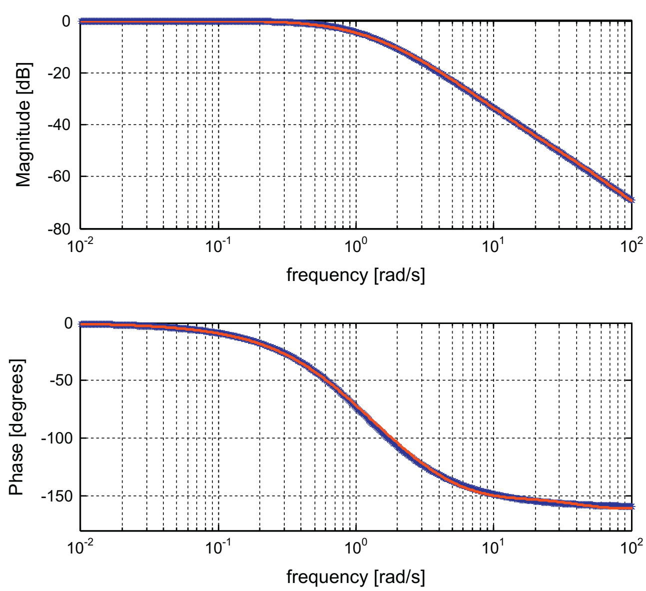

Fig. 11. Frequency response of the FO *Q*-filter (blue dots) and its approximation (red line).

From Eq. (9) we obtain:

$$T_g(t) = T(t) - T_m(t) - T_c \tag{10}$$

where $T_m(t) = J\dot{\omega}(t) + D\omega(t)$.

In Eq. (10), $T(t)$ can be directly and easily computed by current measurements; T_c can be estimated by offline experiments and $T_m(t)$ can be computed through velocity measurements by motor model inversion. Notice that friction (viscous and Coulomb) torques are usually jointly estimated offline using constant speed experiments. Here we included the viscous friction effects into the motor model, and we separately measured the Coulomb friction torque using constant low speed experiments (in which viscous friction effects can be considered negligible).

In this way, the relation between $T_m(t)$ and $\omega(t)$ is given by the following transfer function

$$G(s) = \frac{1}{Js + D} \tag{11}$$

The load mass observer is depicted in Fig. 9, where $G_n^{-1}(s)$ is the inverse (nominal) model of the motor; $Q(s)$ is a fractional order linear filter with unitary gain designed according to [25]. This filter must have relative degree at least 1, in order to guarantee that the observer is described by proper transfer functions; K_{gear} is the transmission ratio; $T_{dist}(t) = T_c + T_g(t)$ is the total disturbance torque.

The design of the filter $Q(s)$ will be explained in detail in Section 6.

In order to implement the scheme of Fig. 9, Coulomb friction value must be estimated by performing experiments with the velocity closed loop controller active and using a small amplitude (about 0.5 cm/s vertical speed) square wave velocity reference signal, so that the viscous friction effect can be considered negligible.

T_C depends on the load weight applied to the manipulator. So, the experiments have been performed with three different load values (14 kg, 39 kg, 74 kg). As an example, in Fig. 10, the experiment with 39 kg is shown. Notice that the current is switching between two values I^+ and I^-, according to the velocity changes from a positive value to a negative one. The current mean value generates the static load balancing torque. This way, for each different load value, the Coulomb friction coefficient can be estimated as follows:

$$T_C = \frac{1}{2}K_t(I^+ - I^-) \tag{12}$$

The estimated values for different load weights are shown in Table 1.

Finally, by linear interpolation of the measured values depending on the current mass estimate value, a function $T_C(M)$ is obtained to be used in the load weight estimator, where the load estimate $\widehat{M}$ is utilized.

The linear part of the model depends on two parameters, namely the total inertia J and the viscous friction coefficient D. The tuning procedure has been carried out in a closed loop (direct method) using different load values. The model parameter estimation followed two steps:

(1) The closed loop system has been excited by band limited white noise reference velocity signal with bandwidth limit at 5 Hz (see Fig. 5 as an example).

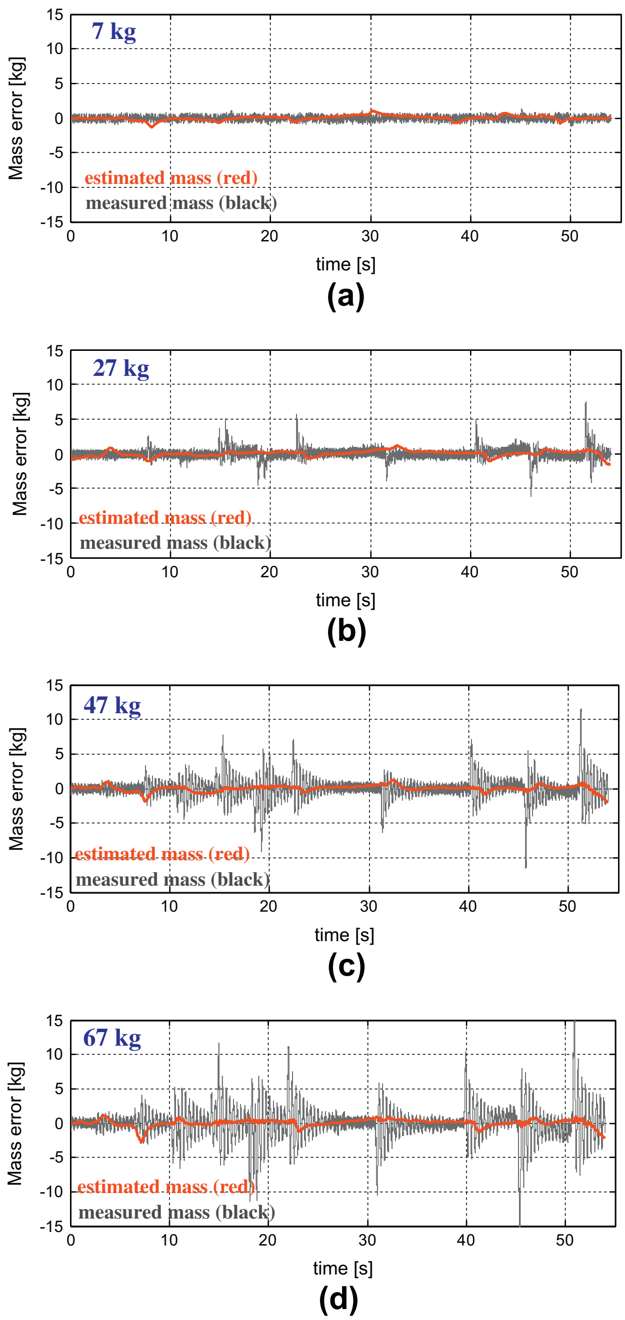

Fig. 13. Comparison between the software sensor error in the mass estimate (red) and the load cell measurement error (gray) in four different operating conditions: (a) 7 kg; (b) 27 kg; (c) 47 kg; and (d) 67 kg.

Table 2
Performance indexes for the load cell and the software sensor.

Load (kg)	Load cell error		Load estimator error	
	MSE (kg^2)	ME (kg)	MSE (kg^2)	ME (kg)
7	0.079	1.35	0.109	1.36
27	0.60	7.48	0.170	1.59
47	2.46	11.55	0.194	1.99
67	6.30	16.6	0.282	2.81

(2) The parameters have been estimated using the measured speed and current by minimization of the following cost function:

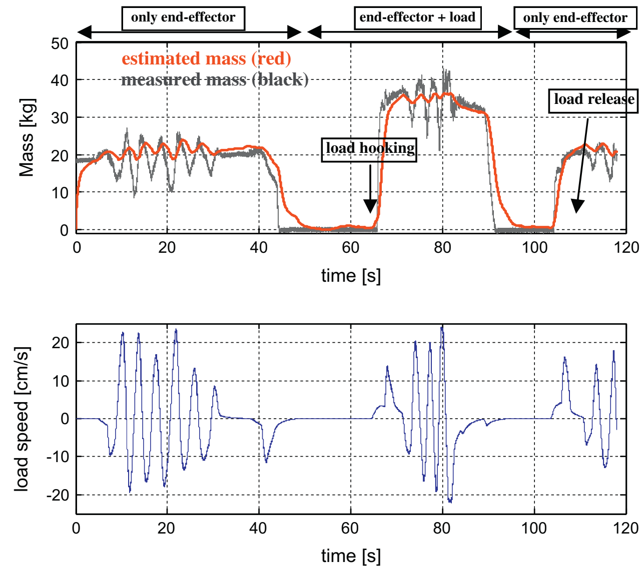

Fig. 14. Example of mass estimation during movement with a varying load. Upper figure: mass values (red-estimated mass; black-measured mass); lower figure: load speed.

$$V(J,D) = \frac{1}{N}\sum_{t=1}^{N}(M - \widehat{M}(t;J,D))^2 \qquad (13)$$

where M is the known load and $\widehat{M}(t;J,D)$ is the estimated load weight for given values of the parameters J and D.

6. Load weight estimator: experimental results

The load mass observer designed and tuned in the previous section has been tested with four different load weights (7 kg, 27 kg, 47 kg, 67 kg) in two different kinds of experiments. During all the tests the resulting estimate is compared with the measurement provided by the load cell usually available on this manipulator.

The first sort of experiment has been performed with the velocity controller active using the same reference signal yet used to validate the controller performances and here depicted in Fig. 12. This reference trajectory is really demanding for the plant, and the load is subject to very different operating conditions including very high acceleration values that are beyond the motor power limit.

The performance has been quantitatively evaluated by means of the following two performance indexes:

(1) The Mean Squared Error (MSE), i.e. the L_2 norm of the difference between the weight estimate (or the load cell measure) $\widehat{M}(t)$ and the true load weight, in order to evaluate the mean performance:

$$\mathrm{MSE} = \frac{1}{N}\sum_{t=1}^{N}(M - \widehat{M}(t))^2 \qquad (14.a)$$

(2) The Maximum Error (ME), i.e. the ℓ_∞ norm of the difference between the estimate (or the measure) and the true weight, in order to evaluate the worst case performance:

$$\mathrm{ME} = \sup_{t\in[1,N]}(M - \widehat{M}(t)) \qquad (14.b)$$

being N the number of samples of the reference signal.

The performance indexes MSE and ME have been calculated for both the load cell mass measure and the nonlinear mass observed.

The filter $Q(s)$ plays a key role in the performance of the load estimator. Specifically, using filters with high relative degree will provide more accurate estimates, according to Eq. (14) but will introduce large delays in the load estimate.

So, according to [25], we used the Fractional Order (FO) Q-filter

$$Q(s) = \frac{1}{\left(1 + \frac{s}{\omega_Q}\right)^{n_Q}} \quad (15)$$

letting n_Q to assume fractional values. In this way, we can obtain a desired attenuation with the smallest phase shift. We choose the value ω_Q = 1.15 rad/s for the cut-off frequency of the Q-filter and we used the relative degree n_Q as a tuning knob. As expected, the error values decrease as n_Q increases, since the response of the filter become smoother. But also the filter transient time become larger and the phase shift introduces further delay. So, we exploit the trade-off between the estimation error and the filter transient time obtaining an optimal value n_Q = 1.78.

Following the rationale described in [25] the frequency response has been identified using N = 1000 data points generated by:

$$Q(j\omega) = \frac{1}{(1 + j0.869\omega)^{1.78}} \quad (16)$$

with $\omega[10^{-2}, 10^{2}]$ rad/s.

In order to approximate the frequency response of $Q(j\omega)$, the following model family has been chosen

$$\widehat{Q}(j\omega) = \frac{\prod_{k=1}^{n}(1 + j\omega\tau_k)}{\prod_{h=1}^{n}(1 + j\omega\tau_h)} \quad (17)$$

The filter identification procedure included also a structural identification stage, performed by cross-validation, which provided a sixth order model

$$\widehat{Q}(s) = \frac{3.5910^{-8}(s + 10000)(s + 6509)(s + 5435)(s + 257.5)(s + 60.99)(s + 20.1)}{(s + 45.49)(s + 43.93)(s + 2.457)(s + 0.8164)(s + 1000)^2} \quad (18)$$

In Fig. 11 the frequency responses (magnitude and phase) for the filter $Q(s)$ (Eq. (16) – blue) and of its approximation $\widehat{Q}(s)$ (Eq. (18) – red) are shown.

Fig. 13a–d shows the comparison between the weight measurement errors, provided by the load cell transducer, and the weight estimate errors given by the mass observer. In Table 2 the performance indexes of Eqs. (14.a) and (14.b) are reported. It can be noticed that the performances of the estimator are similar to those of the load cell with small load and even better at large load values. This phenomenon is due to the large sensitivity of the load cell to large inertial components, since heavy loads show large oscillations during their movement. The vertical component of the acceleration is measured by the load cell, whose measurement is not compensated for this effect. On the contrary, the inertial component is partially compensated by the software estimator since it includes a model of the load dynamics.

A second experiment has been performed to evaluate the performance on a standard working cycle, with varying load conditions. Specifically, the test has been done using the pneumatic equipment for load handling; this is managed by a supervisor enabling the load attach or detach on the basis of the load weight information provided by the estimator instead of the load cell as in the standard manipulator. Correct operation of the pneumatic end-effector is guaranteed if the maximum error is within about 4 kg of the load weight range 0–40 kg.

Fig. 14 (upper figure) shows the comparison between the measured and the estimated load weight during a standard working cycle driven by a human operator: the pneumatic handling equipment (whose weight is about 20 kg) without any load is lifted up and moved up and down for about 30 s. Then, the suction pad is applied to the load (about 17 kg), which gets attached and lifted to place. This operation, which requires the activation of the compressor to obtain vacuum in the suction pad, lasts about 20 s. After a few movements up and down, the load is dropped off on the floor and detached. Finally, the free equipment is raised again and moved up and down. Fig. 14 (lower figure) shows the velocity profile measured during the test.

The performances provided by the mass estimator and the load cell are similar; in particular the mass observer shows a slight delay (especially during the hooking and unhooking phase) due to the presence of the filter $Q(s)$ in the estimation algorithm. On the other side though, in dynamic conditions, it presents lower oscillations in comparison with the load cell mass measure.

7. Concluding remarks

The application of VRFT to the tuning problem of the velocity controller of a DC brushed motor has been successfully completed. The controller shows very good tracking performances and robustness to modifications of the operating and load conditions. The proposed tuning procedure fits the requirements of an end-of-line tuning: it is completely automatic and it is not time consuming, since it can be performed and validated in a very short time, basically the time needed to the acquisition of a single batch of I/O data.

The designed control system, based on the velocity measurement, does not need load weight information for motion control. However, mass information is still necessary for some operating tasks. In order to obtain a real-time load weight estimate, a software sensor has been designed involving a friction compensator for the torque disturbance observer. The weight estimate provided by the observer is precise enough in comparison to load cell measurements.

Acknowledgement

The authors would like to thank Maria G. Perrone, Bakersfield College (USA) faculty, for the useful language review.

References

[1] Savaresi SM, Guardabassi GO. Approximate feedback linearization of discrete time nonlinear systems using virtual input direct design. Syst Control Lett 1997;32:63–74.
[2] Savaresi SM, Guardabassi GO. Approximate I/O feedback linearization of discrete time nonlinear systems via virtual input direct design. Automatica 1998;34:715–22.
[3] Guardabassi GO, Savaresi SM. Virtual reference direct design method: an off-line approach to data-based control system design. IEEE Trans Autom Control 2000;45:954–9.
[4] Guardabassi GO, Savaresi SM. Approximate linearization via feedback – an overview. Automatica 2001;27:1–15.
[5] Campi MC, Lecchini A, Savaresi SM. Virtual reference feedback tuning (VRFT): a new direct approach to the design of feedback controllers. In: Proc of the 39th conference on decision and control; 2000.
[6] Campi MC, Lecchini A, Savaresi SM. Virtual reference feedback tuning for two degree of freedom controllers. Automatica 2002;38:1337–46.

[7] Campi MC, Lecchini A, Savaresi SM. Virtual reference feedback tuning: a direct method for the design of feedback controllers. Int. J Adapt Control Signal Process 2002;16:355–71.
[8] Campi MC, Lecchini A, Savaresi SM. An application of the virtual reference feedback tuning (VRFT) method to a benchmark active suspension system. Eur J Control 2003;9:66–76.
[9] Previdi F, Schauer T, Savaresi SM, Hunt KJ. Data-driven control design for neuroprotheses: a virtual reference feedback tuning (VRFT) approach. IEEE Trans Control Syst Technol 2004;12:176–82.
[10] Previdi F, Ferrarin M, Savaresi SM, Bittanti S. Closed-loop control of FES supported standing up and sitting down using virtual reference feedback tuning. Control Eng Pract 2005;13:1173–82.
[11] Previdi F, Belloli D, Cologni A, Savaresi SM. Virtual reference feedback tuning (VRFT) design of cascade control systems with application to an electro-hydrostatic actuator. In: Proc of the 5th IFAC symposium on mechatronic systems; 2010.
[12] Sjöberg J, De Bruyne F, Agarwal M, Anderson DO, Gevers M, Kraus F, et al. Iterative controller optimization for nonlinear system. Control Eng Pract 2003;11(9):1079–86.
[13] Karimi HR, Yazdanpanah MJ, Patel RV, Khorasani K. Modelling and control of linear two-time scale systems: applied to single-link flexible manipulator. J Intell Rob Syst 2006;45(3):235–65.
[14] Radac MB, Precup RE, Petriu EM, Preitl S. Application of IFT and SPSA to servo system control. IEEE Trans Neural Netw 2011;22(12):2363–75.
[15] Buja G, Menis R, Valla MI. Disturbance torque estimation in a sensorless DC drive. IEEE Trans Indust Electron 1995;42(4):351–7.
[16] Senjyu T, Shingaki T, Uezato K. Sensorless vector control of synchronous reluctance motors with disturbance torque observer. IEEE Trans Indust Electron 2001;48(2):402–7.
[17] Kempf CJ, Kobayashi S. Disturbance observer and feedforward design for a high-speed direct-drive positioning table. IEEE Trans Control Syst Technol 1999;7(5):513–26.
[18] Chen W-H, Ballance DJ, Gawthrop PJ, O'Reilly J. A nonlinear disturbance observer for robotic manipulators. IEEE Trans Indust Electron 2000;47(4):932–8.
[19] Murakami T, Yu F, Ohnishi K. Torque sensorless control in multidegree-of-freedom manipulator. IEEE Trans Indust Electron 1993;40(2):259–65.
[20] Katsura S, Matsumoto Y, Ohnishi K. Modeling of force sensing and validation of disturbance observer for force control. IEEE Trans Indust Electron 2007; 54(1):530–8.
[21] Åström KJ, Wittenmark B. Computer-controlled systems: theory and design. Upper Saddle River (NJ, USA): Prentice Hall; 1997.
[22] Bittanti S, Picci G. Identification, adaptation, learning: the science of learning models from data. Berlin (Germany): Springer; 1996.
[23] Ljung L. System identification. Englewood Cliffs (NJ, USA): Prentice Hall; 1999.
[24] Kenjo T. Electric motors and their controls. Oxford (UK): Oxford Science Publications; 1991.
[25] Chen YangQuan, Vinagre Blas M, Podlubny Igor. Fractional order disturbance observer for vibration suppression. Nonlinear Dyn 2004;38(1–4):355–67.